A Theory of Electron Transfer and Steady-State Optical Spectra of Chromophores with Varying Electronic Polarizability

Dmitry V. Matyushov* and Gregory A. Voth*

Department of Chemistry and Henry Eyring Center for Theoretical Chemistry, University of Utah, 315 S. 1400 E. RM Dock, Salt Lake City, Utah 84112

Received: April 16, 1999; In Final Form: August 20, 1999

Electron transfer (ET) reactions and optical transitions are considered in chromophores with both the dipole moment and the electronic polarizability varying with the transition. An exact solution for reaction free energy surfaces of ET along a reaction coordinate has been obtained in the Drude model for the solute and solvent polarizabilities. The ET surfaces manifest the following effects of a nonzero polarizability variation: they (i) are asymmetric, (ii) have different curvatures at their minima, and (iii) become infinite for reaction coordinates outside a one-sided fluctuation band. The physical origin of these effects is the renormalization of the solute dipole by the solvent reaction field depending on the nonequilibrium solvent configuration. The reorganization energies of ET are substantially different for forward and backward transitions with higher reorganization energy in the state with hider solute polarizability. The dependence of the ET rate on the equilibrium energy gap is quadratic near the rate maximum and is linear at large energy gaps. The energy gap curves are also flatter from the side of exothermic reactions and broader for the state with a higher polarizability. The bandshape analysis of optical transitions is extended to the case of a nonzero polarizability variation.

1. Introduction

Optical spectroscopy and electron transfer (ET) reactions both probe the same elementary process occurring in a molecule (solute): the change in its electronic state. Three major manifestations of such transitions are (i) a variation of the electric field of the solute acting on the surrounding condensed phase (solvent), (ii) a change in the intramolecular nuclear structure of the molecule undergoing electronic transition, and (iii) a change in a set of transition dipoles and energy gaps of virtual transitions to other electronic states of the molecule. The first feature is traditionally related to the solvent effect on spectroscopic and activation parameters.[1] The second effect is responsible for intramolecular reorganization and conformational flexibility of the molecule.[2] The third effect is reflected in the ability of the solute to respond to an external electric field. The intensity of the response is scaled with the polarizability of each electronic state that determines the magnitude and orientation of the induced dipole created at the solute. Here we look at the combined effect of (i) and (iii) addressing the problem of modification of the solute−solvent coupling by the solute electronic polarizability.

The solute electric field polarizes the condensed medium, resulting in an electric (reaction) potential acting on the solute localized charges. For a nonzero polarizability of the solute, the solvent potential deforms the electronic charge distribution producing induced charges acting back on the solvent. This self-consistent action enhances the effective field of the solute and leads to higher solvent reorganization energies of electronic transitions.[3−5] To illustrate this point, consider a dipolar solute possessing the dipole moments m_{0i} in the two ET states labeled as $i = 1, 2$. As is well-known,[6,7] a nonzero solute polarizability α_{0i} results in a renormalization of the solute dipole $m_{0i} \rightarrow m'_{0i}$ increasing its value such that

$$m'_{0i} = m_{0i}/(1 - 2a\alpha_{0i}) \tag{1}$$

Here, $a > 0$ refers to the solvent response function such that the equilibrium chemical potential of solvation μ_i is given by

$$\mu_i = -am_{0i}m'_{0i} \tag{2}$$

As is seen from eq 2, the solvation chemical potential is enhanced by the factor $1/(1 - 2a\alpha_{0i})$ compared to the case of a nonpolarizable solute $\alpha_{0i} = 0$. The solvent reorganization energy defined in terms of equilibrium solvation by the nuclear solvent modes[1,2] should increase as well. The reorganization energy of a polarizable solute is, therefore, higher than the reorganization energy of a nonpolarizable solute.[3−5]

The next question that still needs understanding is how the reorganization parameters are modified if the polarizability *changes* with the electronic transition.[3b,d,8,9] Two qualitative features can be envisioned from the following reasoning. Coupling of the solvent reaction potential to the difference of the solute charge densities in the charge transfer and initial states is associated with the ET reaction coordinate. The free energy invested in creation of a nonequilibrium solvent configuration determines the free energy surface of ET.[1] A nonequilibrium solvent configuration creates a nonequilibrium reaction field that induces charges on the solute. These induced charges may add to, or subtract from, the fixed solute charges. The effective solute−solvent coupling will, therefore, increase or decrease depending on the solvent configuration. Since the solute−solvent coupling is projected into the ET reaction coordinate, solvent fluctuations of the same energy may correspond to different reaction coordinates. This implies an asymmetry of the free energy surfaces of ET. Furthermore, when the polarizability of the solute changes with instantaneous electronic transition, the induced solute dipole changes instantaneously as well. Its interaction with the reaction field of the nuclear subsystem,

10.1021/jp991246x CCC: $18.00
Published on Web 11/20/1999

frozen on the time scale of ET, will be different in the two states. This results in a component of the solvent reorganization energy proportional to the polarizability variation $\Delta\alpha = \alpha_{02} - \alpha_{01}$. These two qualitative predictions of the effect of a nonzero $\Delta\alpha$ on electronic transitions, asymmetry of the energy surfaces and enhancement of the reorganization energy, have motivated our present study.

The aim of this paper is to provide qualitative insights into the effect of the solute polarizability change on the activation and spectroscopic parameters of electronic transitions. General relations are presented below for the activation and reorganization free energies, as well as for the spectral moments and band profiles of optical transitions. Although we use the dielectric continuum model for numerical evaluations, the theory is formulated in terms of the solvent response functions and is, therefore, open to more sophisticated molecular treatments of the solvent response. In section 2, we obtain the exact solution for the free energy surfaces of ET for polarizable solutes and analyze the reorganization parameters and the energy gap law for ET reactions. It is shown that different polarizabilities in the neutral and charge transfer states bring about different reorganization energies and asymmetries of the free energy surfaces. This is projected into an asymmetric free energy gap law for ET: the dependence of the activation energy on the driving force (energy gap law) is found to be less curved and is shallower from the side of exothermic reactions for the state with higher polarizability. The energy gap law of ET becomes increasingly asymmetric with increasing $\Delta\alpha$. A linear dependence on the driving force holds for large energy gaps. In section 3, spectroscopic parameters of optical transitions with $\Delta\alpha \neq 0$ are considered. In section 4 we conclude.

2. Electron Transfer

2.1. Free Energy Surfaces. The concept of reaction free energy surfaces along a reaction coordinate has become a basis for theoretical descriptions of thermally activated and optical electronic transitions of molecules dissolved in condensed phases.[1,2] The procedure of calculating the free energy surfaces is essentially based on the idea of adiabatic separation of different time scales characteristic of the system undergoing the electronic transition.[10] Two steps are usually considered. In the first step, the electronic degrees of freedom of the solute and the solvent are traced out to define the instantaneous (partial) free energies[10c,f,g]

$$\exp[-\beta E_i] = \mathrm{Tr}_{\mathrm{el}}(\exp[-\beta H_i]) \tag{3}$$

where H_i is the Hamiltonian of the system in the ground ($i = 1$) or excited ($i = 2$) states, $\beta = 1/k_{\mathrm{B}}T$, and $\mathrm{Tr}_{\mathrm{el}}$ means the trace over the quantum states of the fast electronic degrees of freedom. The energies E_i are treated as functions of the configuration of the slow nuclear subsystem. The conventional Born−Oppenheimer energies are $\beta \rightarrow \infty$ limits of the free energies E_i. Fluctuations of the nuclear coordinates result in the resonance $E_1 = E_2$ when the electronic transition occurs. The ET free energy surface is therefore defined as the free energy invested in creating a particular mismatch $X = \Delta E = E_2 - E_1$ between the instantaneous free energies E_i. The collective energy gap coordinate X thus becomes a natural choice for the reaction coordinate. The associated free energies $F_i(X)$ are mathematically given by the expression[11,12]

$$\exp[-\beta F_i(X)] = \beta^{-1}\,\mathrm{Tr}_{\mathrm{nuc}}(\delta(X - \Delta E)\exp(-\beta E_i)) \tag{4}$$

Here, $\delta(x)$ is the delta function and $\mathrm{Tr}_{\mathrm{nuc}}$ refers to the integral over the nuclear coordinates of the system. Of course, the formalism outlined above has been used in quite a number of ET theories, both analytical[10,11b,12,13c] and numerical.[4,13] The novel feature of the development in this paper is the explicit inclusion of the variation of the solute polarizability in calculating the free energies $F_i(X)$. The rest of this section is developed in line with the two-step procedure given by eqs 3 and 4.

The model considered here assumes a solute with the dipole moment and polarizability both varying with electronic transition:

$$\mathbf{m}_{01} \rightarrow \mathbf{m}_{02}, \quad \alpha_{01} \rightarrow \alpha_{02} \tag{5}$$

The solute is dissolved in a solvent of molecules bearing the dipole moment $\mathbf{m}$ and the polarizability α. For simplicity, only isotropic solute and solvent polarizabilities are considered. An extension to anisotropic polarizabilities is straightforward in the framework of our formalism.[10f]

The instantaneous free energies E_i of a dipolar polarizable solute in a dipolar polarizable solvent can be derived using the Drude model for induced solute and solvent dipole moments.[14] This approach represents the induced dipoles as fluctuating vectors: $\mathbf{p}_j$ for the solvent molecules and $\mathbf{p}_0$ for the solute. The potential energy of creating a fluctuating induced dipole $\mathbf{p}$ is given by that of a harmonic oscillator, $\mathbf{p}^2/2\alpha$, with the polarizability α appearing as the oscillator mass. The system Hamiltonian H_i is the sum of the solvent−solvent, H_{ss}, and solute−solvent, $H_{0\mathrm{s}}^{(i)}$, parts

$$H_i = H_{0\mathrm{s}}^{(i)} + H_{\mathrm{ss}} \tag{6}$$

In H_i, the permanent and induced dipoles add up resulting in the solute−solvent and solvent−solvent Hamiltonians in the form

$$H_{0\mathrm{s}}^{(i)} = I_i + U_{0\mathrm{s}}^{\mathrm{rep}} - \sum_j (\mathbf{m}_{0i} + \mathbf{p}_0)\cdot\mathbf{T}_{0j}\cdot(\mathbf{m}_j + \mathbf{p}_j) + (1/2\alpha_{0i})[\omega_0^{-2}\dot{\mathbf{p}}_0^{\,2} + \mathbf{p}_0^{\,2}] \tag{7}$$

and

$$H_{\mathrm{ss}} = U_{\mathrm{ss}}^{\mathrm{rep}} - {}^1/_2\sum_{j,k} (\mathbf{m}_j + \mathbf{p}_j)\cdot\tilde{\mathbf{T}}_{jk}\cdot(\mathbf{m}_k + \mathbf{p}_k) + (1/2\alpha)\sum_j [\omega_{\mathrm{s}}^{-2}\dot{\mathbf{p}}_j^{\,2} + \mathbf{p}_j^{\,2}] \tag{8}$$

Here and throughout this paper "0" indicates the solute, $\mathbf{T}_{jk}$ is the dipole−dipole interaction tensor, and $\tilde{\mathbf{T}}_{jk} = \mathbf{T}_{jk}(1 - \delta_{jk})$; $U_{0\mathrm{s}}^{\mathrm{rep}}$ and $U_{\mathrm{ss}}^{\mathrm{rep}}$ stand for repulsion potentials and I_i is the vacuum energy of the ith electronic state. The frequencies ω_0 and ω_{s} characterize electronic excitations of the solute and the solvent, respectively.

The statistical average over the electronic degrees of freedom in eq 3 is equivalent, in the Drude model, to integration over the induced dipole moments $\mathbf{p}_0$ and $\mathbf{p}_j$. The Hamiltonian H_i is quadratic in the induced dipoles and the trace can be calculated exactly as a functional integral[15] over the fluctuating fields $\mathbf{p}_0$ and $\mathbf{p}_j$ (see Appendix A).[10f] The resulting instantaneous free energy

$$E_i = E_{\mathrm{ss}} + E_{0\mathrm{s},i} \tag{9}$$

is composed of the solvent−solvent part, E_{ss} (eq A7 in Appendix A), and the solute−solvent part[16]

$$E_{0s,i} = I_i + U_{0s}^{rep} + U_{0s,i}^{disp} - \mathbf{m}_{0i}\cdot\mathbf{f}_{ei}\cdot\mathbf{R}_p - {}^1/_2\mathbf{m}_{0i}\cdot\mathbf{R}_\infty\cdot\mathbf{f}_{ei}\cdot\mathbf{m}_{0i} - {}^1/_2\mathbf{R}_p\cdot\alpha_{0i}\mathbf{f}_{ei}\cdot\mathbf{R}_p \quad (10)$$

Here $\mathbf{R}_p$ is the reaction field of the solvent nuclear subsystem (eq A9), $\mathbf{R}_\infty$ is the reaction fields created by the induced solvent dipoles (eq A10), and

$$\mathbf{f}_{ei} = [\mathbf{1} - \alpha_{0i}\mathbf{R}_\infty]^{-1} \quad (11)$$

The terms U_{0s}^{rep} and $U_{0s,i}^{disp}$ in eq 10 stand for the solute−solvent repulsion and dispersion potentials, respectively. The terms $\mathbf{R}_\infty$ and $\mathbf{f}_{ei}$ are generally second-rank tensors, with the latter being responsible for the effective enhancement of the solute dipole moment by the reaction field of the solvent induced dipoles.

In principle, both $\mathbf{R}_\infty$ and $\mathbf{R}_p$ depend on the center-of-mass coordinates of the solvent molecules; $\mathbf{R}_p$ also depends on the orientations of the solvent permanent multipoles. In defining the free energy surfaces according to eq 4, we need to include averages over both the $\mathbf{R}_\infty$ and $\mathbf{R}_p$ reaction fields. In such a treatment, the free energy surfaces in eq 4 are obtained by calculating a cumulant expansion in the solute−solvent potential.[3,17] It appears that the second-order cumulants involving dispersion and induction forces are much smaller than the corresponding first-order cumulants.[3c−e] Physically, this means that the reaction field $\mathbf{R}_\infty$ does not vary considerably with fluctuations of the center-of-mass coordinates of the molecules in dense molecular solvents and can be replaced by its average $\langle\mathbf{R}_\infty\rangle$. This is the approximation we adopt in the present paper. The harmonic Drude model for the induced dipoles is equivalent to the linear response approximation (LRA) in which the chemical potential of solvation by the induced solvent dipoles is $-a_e f_{ei} m_{0i}^2$ and the reaction field of the induced dipoles reads

$$\langle R_\infty\rangle_{\alpha\beta} = 2a_e\delta_{\alpha\beta}m_{0i,\beta} \quad (12)$$

Here, a_e stands for the electronic response function and the Greek subscripts denote the Cartesian components of the tensor $\langle\mathbf{R}_\infty\rangle$ and the vector $\mathbf{m}_{0i}$. Under these assumptions, the solute−solvent part of the instantaneous free energies used below have the form

$$E_{0s,i} = I_i + U_{0s}^{rep} + U_{0s,i}^{disp} - a_e f_{ei}\mathbf{m}_{0i}^2 - f_{ei}\mathbf{m}_{0i}\cdot\mathbf{R}_p - {}^1/_2\alpha_{0i} f_{ei}\mathbf{R}_p^2 \quad (13)$$

and

$$f_{ei} = [1 - 2a_e\alpha_{0i}]^{-1} \quad (14)$$

The last, negative contribution to $E_{0s,i}$ in eq 13 is very important for the following development (see also Appendix in ref 3d). It is responsible for the modulation of the force constant of the fluctuations of the solute−solvent coupling by the solute polarizability (see Discussion below). An analogous term appears in the second-order perturbation to the instantaneous Born−Oppenheimer energies (instead of instantaneous free energies used here, see ref 10f) in Kim's description.[10d] In ref 10d, however, the ET free energy surfaces were not calculated and the term $\propto \alpha_{0i}\mathbf{R}_p^2$ was altogether omitted in the subsequent study of ET.[10e]

Equation 13 suggests that it is only the distribution of the inertial (nuclear) reaction field $\mathbf{R}_p$ that is needed in order to perform the statistical ensemble average in eq 4. In the LRA, the chemical potential of solvation of the solute dipole $\mathbf{m}_{0i}$ by the solvent inertial (nuclear) degrees of freedom is $-a_p\mathbf{m}_{0i}^2$, where a_p is the response function of the inertial solvent modes. Then, the distribution function $P(\mathbf{R}_p)$ of the inertial reaction field $\mathbf{R}_p$ is a Gaussian function

$$P(\mathbf{R}_p) = (4\pi a_p k_B T)^{-1/2}\exp[-\beta\mathbf{R}_p^2/4a_p] \quad (15)$$

Equations 13−15 form a complete basis for constructing the free energy surfaces $F_i(X)$ according to eq 4. That this description is consistent is seen from the fact that the ensemble average

$$\exp[-\beta\mu_i] = \int \exp[-\beta E_{0s,i}]\, P(\mathbf{R}_p)\, d\mathbf{R}_p \quad (16)$$

generates the well-known[7] solvation chemical potential of a polarizable dipole (eq 2)

$$\mu_i = -af_i m_{0i}^2 \quad (17)$$

where $a = a_p + a_e$ is the total solvent response function and

$$f_i = [1 - 2a\alpha_{0i}]^{-1} \quad (18)$$

For the instantaneous free energies given by eq 13, the reaction coordinate becomes

$$X = \Delta I_{np} - \Delta\tilde{\mathbf{m}}\cdot\mathbf{R}_p - {}^1/_2\Delta\tilde{\alpha}\mathbf{R}_p^2 \quad (19)$$

Here

$$\Delta\tilde{\mathbf{m}} = f_{e2}\mathbf{m}_{02} - f_{e1}\mathbf{m}_{01}, \qquad \Delta\tilde{\alpha} = f_{e2}\alpha_{02} - f_{e1}\alpha_{01} \quad (20)$$

and the nonpolar ("np") energy gap

$$\Delta I_{np} = I_2 - I_1 + \Delta E^{disp} - a_e(f_{e2}m_{02}^2 - f_{e1}m_{01}^2) \quad (21)$$

consists of the vacuum energy gap and solvation stabilization by dispersion, $\Delta E^{disp} = \langle U_{0s,2}^{disp}\rangle - \langle U_{0s,1}^{disp}\rangle$, and induction forces.

Using eqs 13, 15, and 19, one can carry out integration over $\mathbf{R}_p$ in eq 4, which yields the following integral representation for the ET free energy surfaces

$$\exp[-\beta F_i(X) + \beta F_{0i}] = \int_\infty^{-\infty}\frac{d\xi}{2\pi\beta}C_i(\xi)\exp[\mathcal{F}_i(\xi,X)] \quad (22)$$

Here F_{0i} is the equilibrium free energy of the ET system in the ith state

$$\mathcal{F}_i(\xi,X) = i\xi\,(X - \Delta F_i(\xi)) - (\eta_i/\beta)\, g_i(\xi)\xi^2 \quad (23)$$

and

$$C_i(\xi) = \sqrt{f_i g_i(\xi)/f_{ei}} \quad (24)$$

The exponential function $\mathcal{F}_i(\xi,X)$ in eq 23 is written in the bilinear form standard for the high-temperature limit of the ET rate. There are, however, important distinctions from the well-studied case of zero $\Delta\alpha$. In the first place, the quadratic term

$$(\eta_i/\beta)\, g_i(\xi)\xi^2 \quad (25)$$

depends on the ET state. Here

$$\eta_i = a_p(f_i/f_{ei})\Delta\tilde{\mathbf{m}}^2 \quad (26)$$

and

$$g_i(\xi) = [1 - i\xi/\xi_i]^{-1}, \quad \xi_i = \frac{\beta\Delta\tilde{m}^2}{2\eta_i\Delta\tilde{\alpha}} \tag{27}$$

The function $g_i(\xi)$ multiplying the quadratic term ξ^2 in eq 23 is responsible for a nonlinear asymmetry of the free energy surfaces. The factor $g_i(\xi)$ appears as a result of enhancement of the differential solute dipole $\Delta\tilde{\mathbf{m}}$ by a nonequilibrium inertial reaction field of the solvent due to a nonzero $\Delta\tilde{\alpha}$ (cf. eq 27 to eqs 14 and 18). It is also included into the vertical energy gap $\Delta F_i(\xi)$ (eq 23) as

$$\Delta F_i(\xi) = \Delta I_{np} + g_i(\xi)\Delta F_{p,i} \tag{28}$$

where

$$\Delta F_{p,i} = -2a_p f_i[\Delta\tilde{\mathbf{m}}\cdot\mathbf{m}_{0i} + a_p f_i\Delta\tilde{\alpha}\mathbf{m}_{0i}^2] \tag{29}$$

is the differential free energy stabilization due to the inertial solvent modes. In the case $\Delta\tilde{\alpha} = 0$, $\Delta F_{p,i}$ reduces to the well-known[7b] result

$$\begin{aligned}\Delta F_{p,i} &= -2a_p f f_e \Delta\mathbf{m}\cdot\mathbf{m}_{0i} \\ &= -2(af - a_e f_e)\Delta\mathbf{m}\cdot\mathbf{m}_{0i}\end{aligned} \tag{30}$$

The moments of any order $\langle X^n\rangle_i$ follow directly from eq 22 as derivatives

$$\langle X^n\rangle_i = \frac{1}{(-i)^n}\frac{\partial^n}{\partial z^n}G_i(z)|_{z=0} \tag{31}$$

of the generating function

$$G_i(z) = \exp[F_i(z,0)] \tag{32}$$

This yields ($n \geq 2$)

$$\beta^n\langle(\delta X)^n\rangle_i = \frac{(-)^n(2n)!!}{4}(\beta\lambda_i)\left(\frac{\eta_i\Delta\tilde{\alpha}}{\Delta\tilde{m}^2}\right)^{n-2} \tag{33}$$

For the first cumulant one has

$$\langle X\rangle_i = \Delta F_i \tag{34}$$

where

$$\Delta F_i = \Delta I_{np} + \Delta F_{p,i} \tag{35}$$

The second cumulant

$$\beta\langle(\delta X)^2\rangle_i = 2\lambda_i \tag{36}$$

determines the reorganization energy

$$\lambda_i = \eta_i\left[1 - 2\Delta F_{p,i}\frac{\Delta\tilde{\alpha}}{\Delta\tilde{m}^2}\right] \tag{37}$$

When the solute polarizability is constant, the reorganization energy is the same in both reaction states and is given by the well-known relation[3c,7b]

$$\lambda = (af - a_e f_e)\Delta\mathbf{m}^2 \tag{38}$$

The weak dependence of the preexponential factor $C_i(\xi)$ on ξ can be neglected. The integrand in eq 22 is then an analytic function in the complex ξ-plane except the points of essential singularities at ξ_i when $|F_i| \to \infty$. This observation leads to a very important property of the ET free energy surfaces obtained by rewriting the exponential function $F_i(\xi,X)$ in the form

$$F_i(\xi,X) = -i\xi Y - \Delta_i\frac{\xi\xi_i}{\xi + i\xi_i} \tag{39}$$

Here

$$\begin{aligned}Y &= \Delta F_i - X + \lambda_i/2\gamma_i \\ &= \Delta I_{np} + \frac{\Delta\tilde{m}^2}{2\Delta\tilde{\alpha}} - X\end{aligned} \tag{40}$$

$$\Delta_i = \lambda_i/2\gamma_i \tag{41}$$

and

$$\gamma_i = \eta_i\Delta\tilde{\alpha}/\Delta\tilde{m}^2 \tag{42}$$

Also, in the above notation, $\xi_i = \beta/2\gamma_i$ in eq 27. At $\xi \to \infty$, $F_i(\xi) \to -i\xi Y$ and the integral in eq 22 can be evaluated as a contour integral closed in the upper or lower half-plane depending on the sign of Y. When $\Delta\tilde{\alpha} > 0$ the singularities ξ_i (eq 27) are in the lower half plane. The contour integral closed in the upper half-plane then generates zero for the integral over ξ at $Y < 0$. This means that

$$F_i(X) = \infty \tag{43}$$

at

$$X > X_{max} = \Delta I_{np} + \frac{\Delta\tilde{m}^2}{2\Delta\tilde{\alpha}}, \quad \Delta\tilde{\alpha} > 0 \tag{44}$$

Similarly,

$$F_i(X) = \infty \tag{45}$$

at

$$X < X_{min} = \Delta I_{np} - \frac{\Delta\tilde{m}^2}{2|\Delta\tilde{\alpha}|}, \quad \Delta\tilde{\alpha} < 0 \tag{46}$$

The points X_{max} and X_{min} set up the upper and lower boundaries for the values of the energy gaps between the donor and acceptor electronic states that can be achieved by the nuclear fluctuations of the solvent. At $\Delta\tilde{\alpha} \to 0$ the upper and lower boundaries move to positive and negative infinities, respectively, allowing the whole spectrum of the solvent fluctuations.

For $\Delta\tilde{\alpha} > 0$ and $X < X_{max}$ or $\Delta\tilde{\alpha} < 0$ and $X > X_{min}$ the contour integral necessitates accounting for the essential singularity at ξ_i. The integral over ξ evaluated in Appendix B then yields

$$\begin{aligned}&\exp[-\beta F_i(X) + \beta F_{0i}] = \\ &\quad A_i\sqrt{|\Delta_i/Y|}I_1(\beta\sqrt{|Y\Delta_i|}/|\gamma_i|)\exp[-\beta(|Y| + |\Delta_i|)/2|\gamma_i|]\end{aligned} \tag{47}$$

Here, $I_1(x)$ is the first-order Bessel function of the imaginary argument and the preexponential factor

$$A_i^{-1} = 2|\gamma_i|(1 - e^{-\beta\lambda_i/4\gamma_i^2}) \tag{48}$$

provides the normalization

$$\beta\int_{-\infty}^{\infty} dX \exp[-\beta F_i(X) + \beta F_{0i}] = 1 \tag{49}$$

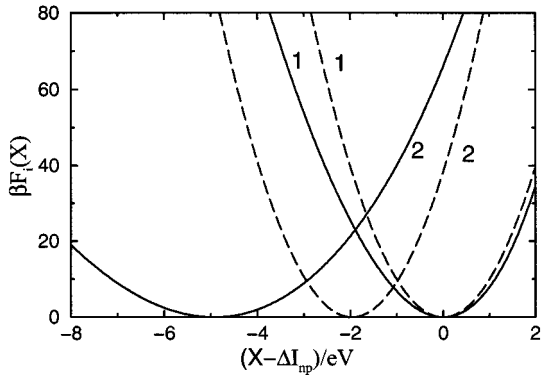

Figure 1. Free energy surfaces $F_i(X)$ (labeled as 1 and 2) for the exited state polarizability $\alpha_{02} = 20$ Å^3 (dashed lines) and $\alpha_{02} = 40$ Å^3 (solid lines). Solute and solvent parameters are $m_{01} = 0$, $m_{02} = 15$ D, $\alpha_{01} = 20$ Å^3, $R_0 = 4$ Å, $\epsilon_s = 2$, $\epsilon_s = 30$; a zero equilibrium energy gap of ET is assumed.

Equation 47 is the exact analytical solution to the problem of calculating the ET free energy surfaces in the presence of a nonzero polarizability variation. Throughout below $\Delta\tilde{\alpha} > 0$ is assumed as the most frequent situation for electronic transitions. When X is not too close to $X_{max,min}$ the inequality $\beta\sqrt{|Y\Delta_i|}/\gamma_i| \gg 1$ allows to use the asymptotic expansion

$$I_1(x) \rightarrow (2\pi x)^{-1/2} e^x, \quad x \rightarrow \infty \tag{50}$$

which yields for the ET free energy surfaces (the preexponential factor is neglected)

$$F_i(X) = F_{0i} + (2\gamma_i)^{-1}(\sqrt{\Delta F_i - X + \lambda_i/2\gamma_i} - \sqrt{\lambda_i/2\gamma_i})^2 \tag{51}$$

At $\lambda_i/2\gamma_i \gg |\Delta F_i - X|$ eq 51 transforms to the standard parabolic form

$$F_i(X) = F_{0i} + \frac{(X - \Delta F_i)^2}{4\eta} \tag{52}$$

Oppositely, when $\lambda_i/2\gamma_i \ll |\Delta F_i - X|$, the linear limit is in order

$$F_i(X) = F_{0i} + \frac{|\Delta F_i - X|}{2\gamma_i} \tag{53}$$

At the boundary $X = X_{max}$, $F_i(X)$ become discontinuous: $F_i(X_{max} - 0) = F_{0i} + \lambda_i/4\gamma_i^2$ and $F_i(X_{max} + 0) = \infty$.

In Figure 1, the ET free energies are plotted for the electronic transition without a polarizability change ($\alpha_{01} = \alpha_{02} = 20$ Å^3, dashed lines) and with the excited polarizability twice as high as that in the ground state ($\alpha_{01} = 20$ Å^3, $\alpha_{02} = 40$ Å^3, solid lines). The calculations are performed for the model spherical solute of the radius $R_0 = 4$ Å with the dipole moments $m_{01} = 0$, $m_{02} = 15$ D. This situation is most close to the charge separation reaction

$$D - A \rightarrow D^+ - A^- \tag{54}$$

The response functions a_e and a_p are taken in the dielectric continuum form[6]

$$a_e = \frac{\epsilon_\infty - 1}{2\epsilon_\infty + 1}\frac{1}{R_0^3} \tag{55}$$

and

$$a_p = \left[\frac{\epsilon_s - 1}{2\epsilon_s + 1} - \frac{\epsilon_\infty - 1}{2\epsilon_\infty + 1}\right]\frac{1}{R_0^3} \tag{56}$$

with the high-frequency, ϵ_∞, and static, ϵ_s, dielectric constants $\epsilon_\infty = 2$ and $\epsilon_s = 30$. Although more accurate algorithms for calculating a_e and a_p are available,[3,12c,13] we are interested here only in qualitative insights into the effect of nonzero $\Delta\alpha = \alpha_{02} - \alpha_{01}$ and a continuum description will suffice for this purpose.

Two salient features are seen from Figure 1. First, the comparison of the dashed-line and solid-line surfaces in the initial state ($i = 1$) shows that the polarizability change brings about an asymmetric shallowness of $F_1(X)$ from the negative X side. The physical origin of this result is clear. The reaction coordinate X reflects the effect of the inertial solvent reaction field on the solute electronic states. Depending on the nonequilibrium nuclear configuration of the solvent, the solute-induced dipole subtracts from or adds to the solute permanent dipole. Therefore, the effective differential solute dipole decreases or increases depending on the solvent configuration resulting in asymmetry of the free energy surfaces. The second effect of a nonzero $\Delta\alpha$ is the broadening of the final ($i = 2$) free energy surface compared to the initial sate ($i = 1$) (see Figure 3). Asymmetry and different curvatures of the free energy surfaces should lead to a nonparabolic dependence of the ET activation energy on the equilibrium free energy gap $\Delta F_0 = F_{02} - F_{01}$ (energy gap law[18−21]) that is considered next.

2.2. Energy Gap Law. The free energies of activation for the forward ($i = 1$, ΔF_1) and backward ($i = 2$, ΔF_2) ET are calculated from eq 47 as

$$F_i^{act} = F_i(X^\ddagger) - F_{0i} \tag{57}$$

where $X^\ddagger$ stands for the position of the activation barrier at the intersection of the two diabatic curves, $F_1(X^\ddagger) = F_2(X^\ddagger)$. The transition state is achieved when the energy gap between the instantaneous free energies is zero and, according to the definition of the reaction coordinate in eq 4, $X^\ddagger = 0$. The activation energy is then given by the simple equation

$$F_i^{act} = \frac{1}{2\gamma_i}(\sqrt{\Delta F_i + \lambda_i/2\gamma_i} - \sqrt{\lambda_i/2\gamma_i})^2 \tag{58}$$

Two types of the energy gap law can be immediately recognized from eq 58. At $|\Delta F_i| \ll \lambda_i/2\gamma_i$ the traditional quadratic dependence is in order

$$F_i^{act} = \frac{(\Delta F_i)^2}{4\lambda_i} \tag{59}$$

In the opposite limit, the linear dependence holds

$$F_i^{act} = \frac{|\Delta F_i|}{2\gamma_i} \tag{60}$$

Experimentally, the energy gap law is monitored by changing the vacuum component of the equilibrium vertical gap ΔF_i through chemical substitution of the donor and/or acceptor units.[18−21] The solvent component of ΔF_i is usually assumed, though not always justly,[22] to be reasonably constant. The quadratic and linear dependence on ΔF_i in eqs 59 and 60 then become the quadratic and linear energy gap laws, respectively. Note also that if X_{max} in eq 44 is negative, no crossing of the diabatic ET surfaces is possible. The activation energy is infinite and no radiationless transitions are induced by the nuclear

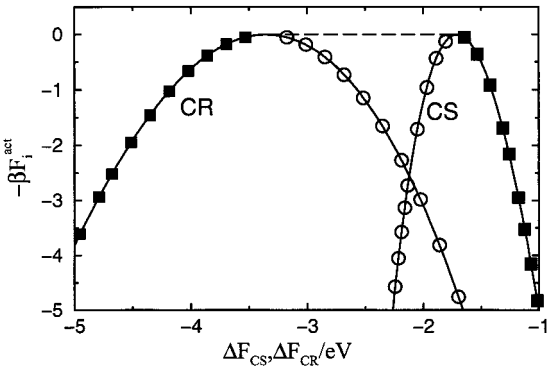

Figure 2. ET energy gap law for the charge separation (CS, $m_{01} \rightarrow m_{02}$, $\Delta F_{CS} = \Delta F_0$) and charge recombination (CR, $m_{02} \rightarrow m_{01}$, $\Delta F_{CR} = -\Delta F_0$) reactions at $\alpha_{01} = 20$ Å^3 and $\alpha_{02} = 40$ Å^3. Parameters are as in Figure 1. Points and the dashed line are drawn to illustrate two possible outcomes of combining CS and CR experimental data in one plot with a common energy gap scale (see the text).

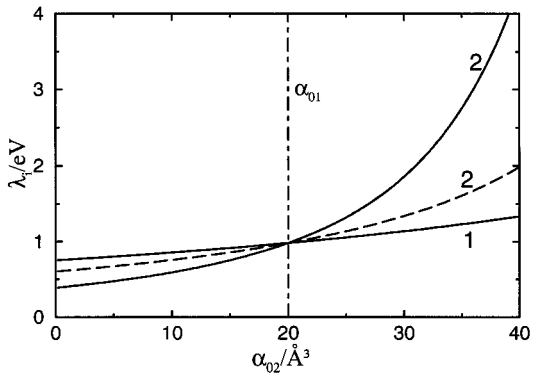

Figure 3. Dependence of the solvent reorganization energy in the initial (1) and charge-separated (2) states on the polarizability of the final state α_{02}. The dashed line indicates the value of η_2 from eq 26. Other solute and solvent parameters are as in Figure 1.

TABLE 1: Ground State Polarizability (α_1) and Trace of the Tensor of Polarizability Variation (1/3) Tr[$\Delta\alpha$] for Several Optical Dyes and Charge Transfer Complexes

chromophore	α_1/Å^3	(1/3)Tr [$\Delta\alpha$]/Å^3	ref
anthracene	25	17	24a
2,2′-bypyridine-3,3′diol	21	11	24d
bis(adamantylidene)	42	29	24c
1-(dimethylamino)-2,6-dicyano-4-methylbenzene	22	35	24b
tetraphenylethylene	50	38	32a
$[(C)_5Fe^{II}CNOs^{III}(NH_3)_5]^-$		57	32c
$(NC)_5Os^{II}CNRu^{III}(NH_3)_5]^-$		(190)317[a]	32d
		310[b]	32e

[a] For two different charge-transfer transitions. [b] Obtained with the local field correction factor $f = 1.3$.

solvent fluctuations. Other activation mechanisms should be included for the reaction to occur.

Figure 2 shows the activation energy of the forward (charge separation, CS) reaction vs $\Delta F_{CS} = \Delta F_0$ and backward (charge recombination, CR) reaction vs $\Delta F_{CR} = -\Delta F_0$ for the transition $m_{01} = 0 \rightarrow m_{02} = 15$ D and $\alpha_{01} = 20$ Å$^3 \rightarrow \alpha_{02} = 40$ Å^3. Two important effects of nonzero $\Delta\alpha$ manifest themselves in Figure 2. First, in contrast to the case of zero $\Delta\alpha$, the maxima of the CS and CR curves do not coincide. Second, the CR curve is broader and shallower from the side of negative energy gaps compared to the CS curve.

The energy gap law for thermally activated ET reactions is often obtained by superimposing CS and CR data on a common scale of ΔF_0.[18] For such a procedure, depending on the energy range studied, two outcomes are predicted by the present theory. For a narrow range of ΔF_{CS} and ΔF_{CR} values close to zero, the intersection of two curves (illustrated by circles in Figure 2) may occur. Such a behavior was indeed observed in ref 18b for a series of porphyrin−quinone diads. Note that maxima of the CS and CR curves get closer to each other with decreasing solvent polarity and, in fact, no curve crossing was seen for the same systems in benzene as a solvent.[18b] When the normal region of CS is combined with the inverted region for CR, another scenario is possible. The two branches (shown by squares in Figure 2) fitted by a single curve (the dashed line in Figure 2) result in a plateau in the energy gap law (a picture reminiscent of this behavior can be seen in Figure 4 of ref 18c).

2.3. Reorganization Energy. In traditional theories of ET the reorganization energy is responsible for two important links: (i) between the vertical *internal* energy gap and the equilibrium *free* energy gap and (ii) between the curvature of the ET free energy surfaces and the energetic intensity of the solvent fluctuations measured by widths of optical spectral lines. These two connections are frequently used as means to define the reorganization energy. In the first route, the reorganization energy is given through the vertical energy gaps corresponding to optical transitions with the energies $\hbar\omega_i$ ($i = 1$ for absorption and $i = 2$ for emission)[4]

$$\lambda_1 = |\hbar\omega_1 - \Delta F_0| \qquad \lambda_2 = |\hbar\omega_2 + \Delta F_0| \qquad (61)$$

The second route is through the mean-squared fluctuation of the nuclear subsystem projected into the reaction coordinate (eq 36).[4,13c,d] The two definitions are equivalent for parabolic ET free energy surfaces, but lead to different results for nonparabolic $F_i(X)$. There is therefore no unique definition of λ_i in the latter case[12c,13d,23] and one of the two routes should be chosen.

We favor the second definition (eq 36) for the following reasons. First, the calculation or experimental probing of the vertical energy gaps involves highly nonequilibrium final states that may be affected by nonlinear solvation and/or asymmetry of the free energy curves owing to differing polarizabilities of the ET states. Second, the second cumulant $\langle(\delta X)^2\rangle_i$ is often available from computer simulations[5,8,13e] and can be exactly calculated in our present model (eqs 36 and 37).

Electronic excitations usually result in higher polarizabilities of the excited state $\alpha_{02} > \alpha_{01}$.[24] Therefore, for positively solvatochromic dyes with $m_{02} > m_{01}$ one has $\Delta F_{p,i} < 0$ in eq 37 and excitation leads to a higher reorganization energy. This is illustrated in Figure 3 where we have plotted λ_i against α_{02}. As is seen, the reorganization energy approximately doubles with excitation when the excited-state polarizability is about 50% higher than the ground-state value. Such polarizability differences are not uncommon for optical chromophores[24] (see Table 1) and we will discuss this result in the application to optical spectroscopy in the next section. The effect of the negative polarizability variation is much weaker and λ_2 is only slightly smaller than λ_1. An opposite dependence of the reorganization energy on the polarizability difference to that given here was reported in ref 8. The reorganization energy computed from simulations via eq 36 falls from 0.86 eV for a nonpolarizable solute ($m_{01} = 5.4 \rightarrow m_{02} = 10.7$ D, $\alpha_{01} = \alpha_{02} = 0$) to 0.43 eV for the transition with the positive polarizability change ($\alpha_{01} = 0.06 \rightarrow \alpha_{02} = 3.21$ Å^3) and the same dipoles. Since the ground-state polarizability is close to zero, that result is also at odds with several previous studies.[3−5]

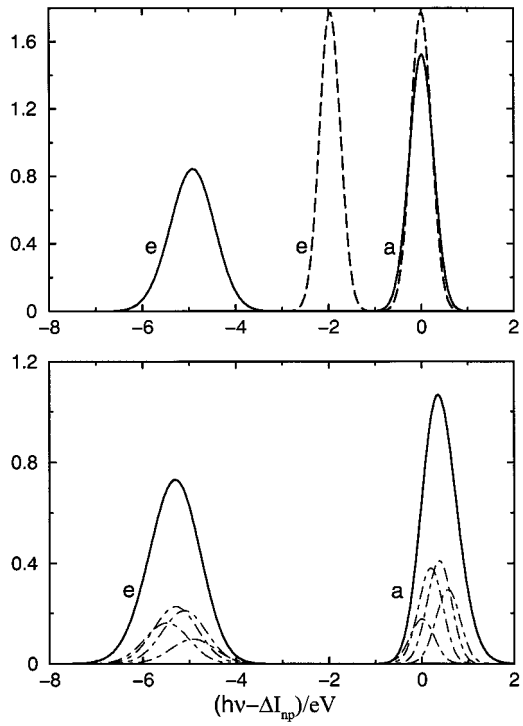

Figure 4. Normalized absorption (a) and emission (e) spectra for $\alpha_{01} = \alpha_{02} = 20$ Å^3 (dashed lines) and $\alpha_{02} = 40$ Å^3 (solid lines). The upper panel shows solvent-broadened lines and the lower panel shows the vibronic envelopes calculated according to eq 69. The dash−dotted lines in the lower panel indicate the four first vibronic components of the sum in eq 69. The solvent and solute parameters are as in Figure 1; $\lambda_v = 0.4$ eV, $\hbar\omega_v = 0.2$ eV.

3. Optical Spectra

Bandshapes of inhomogeneously broadened optical lines can be obtained directly from ET energy surfaces. Normalized ($\int I_i(\omega)\, d\omega = 1$) intensities ($\Delta\alpha > 0$)

$$I_i(\omega) = \beta\hbar A_i\sqrt{\Delta_i/Y(\omega)}I_1(\beta\sqrt{Y(\omega)\Delta_i}/\gamma_i) \times \exp[-\beta(Y(\omega) + \Delta_i)/2\gamma_i] \quad (62)$$

of absorption ($i = 1$) and emission ($i = 2$) transitions follow from the free energy surfaces $F_i(X)$ given in eq 47 by replacing the reaction coordinate X with the energy $\hbar\omega$ of the incident light. If the spectral line can be fitted to a Gaussian, the band maximum

$$\hbar\omega_i = \Delta F_i \quad (63)$$

and the width

$$\sigma_i^2 = 2k_B T\eta_i\left[1 - 2\Delta F_{p,i}\frac{\Delta\tilde{\alpha}}{\Delta\tilde{m}^2}\right] \quad (64)$$

follow from eqs 35 and 36. For a non-Gaussian line, ΔF_i and σ_i^2 give the first and second spectral moments, respectively. The general effect of a positive polarizability change $\Delta\alpha > 0$ is to enhance the solvent-induced shift of emission bands and to broaden bands for both absorption and emission, with a stronger broadening of emission lines. This is illustrated in Figure 4 where we show the normalized intensities $I_i(\omega)$ for a model positively solvatochromic ($m_{02} > m_{01}$) dye (parameters are as in Figure 1) for $\Delta\alpha = 0$ and $\Delta\alpha = 20$ Å^3. Broader emission lines are seen for both the solvent-broadened lines (the upper panel) and for the vibrational envelopes (the lower panel, eq 69 below).

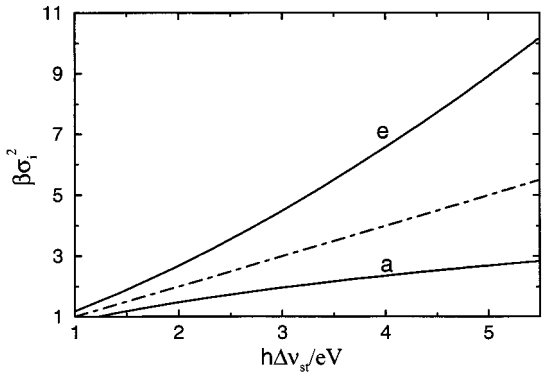

Figure 5. Dependence of absorption (a) and emission (e) widths on the Stokes shift obtained by changing the static solvent dielectric constant in the range $\epsilon_s = 3-65$. The dash−dotted line indicates the equality $\hbar\Delta\omega_{st} = 2\lambda$ valid for $\Delta\alpha = 0$.

The solvent-induced Stokes shift

$$\hbar\Delta\omega_{st} = \hbar\omega_1 - \hbar\omega_2 = 2a_p\Delta\tilde{\mathbf{m}}\cdot[f_2\mathbf{m}_{02} - f_1\mathbf{m}_{01}] + 2a_p^2\Delta\tilde{\alpha}[(f_2 m_{02})^2 - (f_1 m_{01})^2] \quad (65)$$

is now the sum of two contributions: one arising from the variation of the solute dipole (the first summand) and one due to the polarizability change (the second summand). The Stokes shift is hence nonzero even if the charge distribution does not change in the course of the transition ($m_{02} = m_{01}$). A term similar to the second summand in eq 65 appears also in the reorganization energy calculations by Liu and Newton combining the ab initio electronic structure with self-consistent field of nonspherical dielectric cavities.[25] Our exact equation for the Stokes shift differs from the relation given by Kim[10d] due to several approximations employed there. In the limit $\Delta\alpha = 0$, eq 65 is identical to the classical Liptay result,[7b] whereas Kim's equation is not.

One of the consequences of nonzero $\Delta\alpha$ is that the relation

$$\hbar\Delta\omega_{st} = \beta\sigma^2 \quad (66)$$

valid for linear solvation response and $\Delta\alpha = 0$ does not hold any more. In Figure 5, the widths $\beta\sigma_i^2$ are plotted vs the Stokes shift obtained by varying the static dielectric constant of the solvent in the range $\epsilon_s = 3-65$. The absorption width deviates downward from the unity slope line predicted by eq 66 while the emission width goes upward. The opposite behavior follows from nonlinear solvation effects:[23] the absorption width deviates upward from eq 66 and the emission width goes downward. This is because nonlinear solvation results in narrowing of emission lines in contrast to the broadening effect of $\Delta\alpha > 0$. The two effects, therefore, tend to compensate each other in the dependence of $\beta\sigma_i^2$ vs $\hbar\Delta\omega_{st}$, although the effect of the polarizability variation is stronger.

Asymmetry of the free energy surfaces $F_i(X)$ (Figure 1) does not manifest itself in optical bandshapes for the solute and solvent parameters considered here. Deviations from the Gaussian bandshape can be measured by the parameter

$$s_i = \lambda_{wi}/\lambda_i \quad (67)$$

reflecting the difference between the reorganization energy λ_i obtained from the Gaussian width σ_i and the reorganization energy λ_{wi} extracted from the width $\sigma_i(1/2)$ measured at the level

of half band intensity

$$\lambda_{wi} = \frac{\beta\sigma_i(1/2)^2}{16\ln(2)} \tag{68}$$

For the calculations shown in Figures 3 and 5, the parameters s_i are very close to unity, indicating that the optical lines can be fitted to Gaussian functions. Higher polarizability changes are needed for the asymmetry effect to be seen in optical bandshapes. Note also that in many cases the $\Delta\alpha$ tensor is highly anisotropic.[24] A substantial component of $\Delta\alpha$ along the direction of charge transfer may considerably enhance the band asymmetry. Since consideration of real systems is necessary for quantifying this effect, we refrain here from speculating on this point.

For a complete description of the spectral bandshape one needs to include the influence of intramolecular vibronic excitations. In the model of one quantum ($(\lambda_v/\hbar\omega_v)$ cosech$(\beta\hbar\omega_v) \ll 1$), intramolecular (skeletal) vibrational mode with the frequency ω_v and the vibrational reorganization energy λ_v one gets[2c,22,26,27]

$$I_i(\omega) = \beta\hbar A_i\, e^{-S}\sum_{n=0}^{\infty}\frac{S^n}{n!}\sqrt{\frac{\Delta_i}{Y_n(\omega)}}I_1(\beta\sqrt{Y_n(\omega)\Delta_i}/\gamma_i) \times \exp[-\beta(Y_n(\omega)+\Delta_i)/2\gamma_i] \tag{69}$$

Here

$$Y_n = \Delta F_i + \lambda_i/2\gamma_i \pm n\hbar\omega_v - \hbar\omega \tag{70}$$

$S = \lambda_v/\hbar\omega_v$, and "+" and "−" refer to absorption and emission, respectively. The transition frequency is nonzero only if the light frequency is confined by the one-sided band

$$\hbar\omega < \hbar\omega_{max}^{(n)} = \Delta F_i + \lambda_i/2\gamma_i \pm n\hbar\omega_v \tag{71}$$

For absorption transitions, the boundary $\omega_{max}^{(n)}$ blue-shifts with n and all vibronic transitions can effectively contribute to the bandshape. Oppositely, for emission transitions, the band boundary red-shifts with n and starting with n of the order of $S + \lambda_i/2\gamma_i\hbar\omega_v$ the corresponding vibronic excitations contribute increasingly less to the band intensity.

The first spectral moment calculated from eq 69, is equal to $\Delta F_i \pm \lambda_v$. The solvent-induced shift ΔF_i can thus be measured provided λ_v is available from independent sources. The parameters λ_i, γ_i, and ω_v are usually unknown and should be considered as fitting parameters of the bandshape analysis. Yet the coefficients γ_i and the reorganization energies λ_i are not independent as

$$\frac{\lambda_1}{\gamma_1^3} = \frac{\lambda_2}{\gamma_2^3} \tag{72}$$

$$(2\gamma_1)^{-1} = 1 + (2\gamma_2)^{-1} \tag{73}$$

and

$$\frac{\lambda_2}{\gamma_2} - \frac{\lambda_1}{\gamma_1} = 2\hbar\Delta\omega_{st} \tag{74}$$

These relations can be used as a consistency test of the bandshape analysis. Also, when the dispersion component of the spectral shift is negligible, there is a linear correlation between λ_i/γ_i and the energy of the band maximum such that

$$\frac{\lambda_i}{\gamma_i} = \frac{\Delta\tilde{m}^2}{\Delta\tilde{\alpha}} + 2(I_2 - I_1) - 2\hbar\omega_i \tag{75}$$

The factors f_{ei} in $\Delta\tilde{m}$ and $\Delta\tilde{\alpha}$ are commonly close to unity and the intercept of the plot λ_i/γ_i vs $\hbar\omega_i$ can be used as a measure of $\Delta m^2/\Delta\alpha$.

4. Discussion

Underlying the theoretical treatment presented here is the idea that the charge distribution induced on the solute by a nonequilibrium solvent reaction field changes instantaneously with electronic transition if the solute polarizability is different in the two ET states. A Franck−Condon transition changes not only the solute−solvent interaction potential linear in the solvent reaction field $\mathbf{R}_p$ but also the solute polarization energy quadratic in $\mathbf{R}_p$ (eq 13). The instantaneous energy gap between the donor and acceptor states in then a bilinear function in the Gaussian field $\mathbf{R}_p$ (eq 15). The problem of calculating the ET free energy surfaces from the instantaneous free energies E_{0i} is, therefore, formally equivalent to that of two displaced oscillators with different force constants. The corresponding Hamiltonian with the classical nuclear mode q reads

$$H_i = H_{0i} + C_i q + {}^1/_2\omega_i^2 q^2 \tag{76}$$

Radiationless transitions between the surfaces defined by eq 76, usually associated with Duschinsky rotation of normal modes,[28] have been considered in numerous studies focusing mostly on the case quantum nuclear modes.[29] Equation 47 derived here for the particular problem of the solute polarizability effects on electronic transitions gives, at the same time, the exact solution of the Duschinsky rotation problem with classical normal modes. Note that the Franck−Condon factor in the Golden Rule expression for the transition probability is given by eq 47 with $X = 0$.

The model of two displaced parabolas with different curvatures has been actively employed in application to ET by Kakitani and Mataga.[30] However, as first noticed by Tachiya,[31] projection of thermal bath oscillators with different force constants onto one collective transition coordinate $\propto (H_2 - H_1)$ should result both in different curvatures at equilibria and asymmetries of the corresponding free energy surfaces. These are indeed the features reflected by the present model. The interaction of the differential induced charge with the inertial nuclear field frozen on the electronic time scale results in the following qualitative effects: (i) the solvent reorganization energies in the initial and final ET states are different, (ii) the ET free energy curves are asymmetric, and (iii) the range of reaction coordinates is limited by the upper boundary at $\Delta\alpha > 0$ and by the lower boundary at $\Delta\alpha < 0$. The ET free energies are infinite outside the corresponding fluctuation bands. The magnitudes of these effects are governed by the difference of polarizabilities in the final and initial states, $\Delta\alpha$. Unfortunately, measurement[32] and calculation[33] of $\Delta\alpha$ is still a challenge and polarizabilities in both ground and excited states are known only for a few optical chromophores. Recent results of Stark spectroscopy[24b−d,32] indicate that polarizability may vary substantially for many optical chromophores and charge-transfer complexes. To provide the reader with a perception of magnitudes involved, Table 1 shows some examples of polarizability changes taken from the recent Stark spectroscopy literature.[24b−d,32] Noteworthy is a very large polarizability change for binuclear

charge-transfer complexes. Even higher polarizability variations occur in polyenes.[32a,34]

The Marcus theory of ET[1] predicts a parabolic dependence of the ET activation energy on the ET driving force ΔF_0. Such an idealized behavior has, however, never been observed for real ET systems. Although bell-shaped curves are now documented for charge shift,[19] charge separation,[20] and charge recombination[21] reactions, all observed energy gap laws are substantially asymmetric. Basically, two explanations of this asymmetry have been proposed in the literature. The first approach addresses the problem from the viewpoint of the donor−acceptor supermolecule. It assigns the observed asymmetry to intramolecular vibronic excitations. Vibrational excitations accommodate the energy of exothermic reactions making the energy gap curves shallower in the inverted region of ET. This model predicts a mirror symmetry between forward and backward ET: the activation energy of a forward reaction, $\Delta F_1(\Delta F_0)$, should coincide with the activation energy of the backward reaction, $\Delta F_2(-\Delta F_0)$, at the inverted energy gap. This prediction seems, however, to contradict experiments showing very different energy gap laws for CS and CR reactions.[30] On the basis of this observation, Kakitani and Mataga[30] suggested an alternative mechanism addressing the problem from the viewpoint of solvent properties. Their model attributes asymmetry of the energy gap curves to dielectric saturation of the solvent in the charge-separated state. Subsequent computer simulations and integral equation studies of polar solvation showed, however, that the saturation needed to produce the observed asymmetry is hard to achieve in liquid solvents.[13,35] Alternative explanations of the flattening of the energy gap plots involve transient effects of nonequilibrium occupation of the initial and final ET states[36] and spatial distribution of the reactants. The latter mechanism concerns only intermolecular ET.[30c]

In terms of this classification, our present model addresses the problem of asymmetric energy gap curves from the viewpoint of the combined effect of the solute and solvent properties. We assign the origin of the asymmetry of the free energy surfaces of ET to the effect of the solute polarizability varying in the course of electronic transition. This intramolecular *solute* property is coupled to the *solvent* reaction field, thus enhancing or diminishing the solute−solvent coupling depending on the solvent configuration. This differential effect is projected into asymmetric free energy curves with the curvature lower for the state with a higher solute polarizability. The present theory thus predicts different energy gap laws for CS and CR reactions even for intramolecular electronic transitions in rigid donor−acceptor complexes. The qualitative result is that both the CS and CR curves are flatter in the inverted region compared to the normal region of ET and the state with higher polarizability has a broader energy gap dependence. Because of different polarizabilities in the initial and final ET states the maxima of CS and CR energy gap curves are shifted relative to each other. This may result in crossing of the CS and CR curves superimposed in one plot with common energy gap scale or in appearance of a plateau in the near-to-activationless region.

An important result of the present model is the existence of the *linear* energy gap law that holds for relatively large energy gaps (eq 60). The linear dependence of the activation energy on the equilibrium energy gap has indeed been reported for intermolecular[37a−c] as well as intramolecular[27c,37d,e] organic systems, in binuclear complexes,[2c,38] and in charge transfer crystals.[39] It is commonly explained in terms of the weak coupling limit of the theory of vibronic bandshapes yielding the linear-logarithmic dependence $\propto \Delta F_i \ln \Delta F_i$ on the vertical energy gap ΔF_i.[2c,26,27c] The strictly linear dependence $\propto \Delta F_i$ arising from a nonzero polarizability difference may provide an alternative explanation of this phenomenon. In fact, the switch of in the energy gap law from the quadratic to linear dependence happens in passing from weakly coupled[22,37a] to strongly coupled[37a−c] ion pairs. In the latter case, the polarizability may change considerably with charge transition.

Both vibrational envelopes and solvent-broadened optical lines show vastly different widths for emission and absorption spectra with a nonzero $\Delta\alpha$ (Figure 4). Although the numerical examples used in this paper have shown only a very moderate asymmetry of optical bands, some general insights into the effect of the polarizability change on band profiles are relevant here.

The conventional procedure attributes all asymmetry of optical bands to excitations of vibronic states. These transitions are especially effective on blue wings of absorption lines and red wings of emission lines making absorption spectra broader on the right side from the maximum and emission spectra broader on the left side from the maximum. However, the mirror symmetry between absorption and emission lines[40] still holds when vibronic transitions are involved. The polarizability effect is more uniform: both absorption and emission spectra get broader on their red wings as a result of $\Delta\alpha > 0$. Therefore, the two asymmetries, vibronic and polarization, add up on the red side of emission lines making them more asymmetric. In contrast, the polarizability asymmetry on the red side of absorption lines compensates the asymmetry from vibronic transitions on the blue side making absorption lines more symmetric. The mirror symmetry consequently breaks down.

Mathematically this is expressed by the spectroscopic skewness parameter[11a]

$$\kappa_1 = \frac{\langle(\omega - \langle\omega\rangle_i)^3\rangle}{\langle(\omega - \langle\omega\rangle_i)^2\rangle^{3/2}} \tag{77}$$

For intramolecular vibrations the parameter

$$\kappa_1 = \pm[S(\coth(\beta\hbar\omega_v/2))^3]^{-1/2} \tag{78}$$

is positive for absorption ("+") and negative for emission ("− ").[11a] On the other hand, for solvent-induced broadening κ_1 is always negative for $\Delta\alpha > 0$

$$\kappa_1 = -\frac{6}{\sqrt{2\beta\lambda_i}}\frac{\eta_i\Delta\tilde{\alpha}}{\Delta\tilde{m}^2} \tag{79}$$

indicating that emission and absorption of photons of lower energy is more preferable than photons of higher energy.

A considerable difference in the curvatures of the ET free energy surfaces at their minima (Figure 2) is an important result of the present study. The classical Marcus theory[1] assumes equal curvatures in the initial and final states. This assumption has been challenged in terms of nonlinear solvation effects.[13,30,35] The physical background of the different effects of solvation nonlinearity and solute polarizability can be explained by the following qualitative model.

The free energy $F(P)$ invested in creation of a nonequilibrium solvent polarization P can be expressed as a series in even powers of P with the two first terms as follows

$$F(P) = a_1P^2 + a_2P^4 \tag{80}$$

where a_1, $a_2 > 0$. The interaction energy of the solute field

with the solvent polarization, U_{0s}, is linear in P

$$U_{0s} = -bP, \quad b > 0 \tag{81}$$

For weak solute−solvent interactions, deviations from zero polarization of the solvent are small and one can keep only the first harmonic term in eq 80. Anharmonic higher order terms gain importance for stronger solute−solvent couplings and $a_2 \neq 0$ in eq 80. The nonequilibrium solvent polarization can be considered as an ET reaction coordinate. The curvature of the corresponding free energy surface is

$$F''(P_0) = 2a_1 + 12a_2P_0^2 \tag{82}$$

at the minimum point P_0 defined by the condition $F'(P_0) = b$. Equation 82 indicates that nonlinear solvation effects, usually associated with dielectric saturation, enhance the curvature compared to the linear response result $F'' = 2a_1$. This leads to a decrease in the solvent reorganization energy which is relatively small as the effect arises from anharmonic expansion terms.

If the solute polarizability is nonzero, the solute−solvent interaction energy attains the energy of solute polarization that is quadratic in P

$$U_{0s} = -bP - cP^2, \quad c > 0 \tag{83}$$

The total system energy $F(P) + U_{0s}$ includes, therefore, the quadratic in P term with the coefficient $(a_1 - c)$. This quadratic term initiates a revision of the frequency of solvent fluctuations driving ET. The curvature of harmonic surfaces decreases, producing higher reorganization energies. Since the solute polarizability contributes already to the harmonic term, its effect on the reorganization energy is stronger than that of nonlinear solvation. The nonlinear solvation and solute polarizability effects tend to compensate each other.

Due to the solute polarization term $-cP^2$ in eq 83 the instantaneous energy gap between the two electronic states is a bilinear function of P with a negative second derivative for $\Delta\tilde{\alpha} > 0$ and a positive second derivative for $\Delta\tilde{\alpha} < 0$. The range of accessible reaction coordinates is thus limited by the upper boundary in the former case and by the lower boundary in the latter case. As states with X outside those ranges are thermodynamically forbidden, the ET free energy surfaces $F_i(X)$ become infinite for $X > X_{max}$ at $\Delta\tilde{\alpha} > 0$ and for $X < X_{min}$ at $\Delta\tilde{\alpha} < 0$ (eqs 43−46). The probabilities of such fluctuations are zero and the spectral intensities are zero as well for $\hbar\omega \geq X_{max}$ at $\Delta\tilde{\alpha} > 0$ and for $\hbar\omega \leq X_{min}$ at $\Delta\tilde{\alpha} < 0$. There is also no crossing of the diabatic ET surfaces at $X_{max} < 0$. A nonzero variation of the solute polarizability, therefore, produces a one-sided band for thermal and optical excitation of charge transfer complexes. The existence of a band edge should considerably skew an optical band whenever its maximum gets closer to the edge. For $\Delta\tilde{\alpha} > 0$ and $\Delta\tilde{m} > 0$ optical bands red-shift from ΔI_{np} with increasing solvent polarity, thus moving away from the band edge. On the other hand, for negatively solvatochromic dyes with $\Delta\tilde{\alpha} > 0$ and $\Delta\tilde{m} < 0$, bands shift closer to their edges with increasing solvent polarity. Stronger band asymmetries should be expected in such cases.

The free energy surfaces of ET should satisfy the linear relation[4,11b−e,12c,13d]

$$F_2(X) = F_1(X) + X \tag{84}$$

The exact solution given by eq 47 indeed obeys this condition. It can be proved by noticing that the ratio Δ_i/γ_i^2 is the same in both ET states according to eq 72. Therefore, the Bessel function and the preexponential factor in eq 47 cancel out in $\Delta F(X) = F_2(X) - F_1(X)$ and one gets

$$\Delta F(X) - \Delta F_0 = -Y + \frac{\Delta_2}{2\gamma_2} - \frac{\Delta_1}{2\gamma_1} \tag{85}$$

Substitution of the parameters yields eq 84.

The solvent reorganization energy λ_i obtained in the present paper is the product of two terms: (i) η_i that depends on the solute polarizability in the ith state and (ii) the factor $1 - 2\Delta F_{p,i}\Delta\tilde{\alpha}/\Delta m^2 > 0$ that scales as the polarizability difference $\Delta\tilde{\alpha}$ (see eq 37). The effect of the solute polarizability on η_i is relatively small (Figure 3) and has been, in fact, previously included.[3] It is the polarizability *variation*, and correspondingly the factor $1 - 2\Delta F_{p,i}\Delta\tilde{\alpha}/\Delta m^2$, that makes the main contribution to the reorganization energy change with electronic transition. This factor has not been included in previous studies and is a principle result of the present theory.

Acknowledgment. This research has been supported by the Office of Naval Research (N00014-97-0265). Useful discussions with David Reichman are gratefully acknowledged.

Appendix A

The trace over the fluctuating dipoles $\mathbf{p}_j$ and $\mathbf{p}_0$ in eq 3 can be represented by a functional integral[14b,d,15]

$$\mathrm{Tr}_{el}(\exp[-\beta H_i]) = \int D\mathbf{p}_0 \prod_j D\mathbf{p}_j \exp(-\hbar^{-1}S_{0s}[\mathbf{p}_0,\mathbf{p}_j] - \hbar^{-1}S_{ss}[\mathbf{p}_j]) \tag{A1}$$

Here S_{0s} and S_{ss} are the Euclidean actions

$$\beta\hbar S_{0s} = {}^1/_2\sum_n \mathbf{m}_0\cdot\mathbf{T}_{0j}\cdot(\mathbf{p}_{j0} + \mathbf{m}_j) - \sum_j \mathbf{p}_{00}\cdot\mathbf{T}_{0j}\cdot\mathbf{m}_j \tag{A2}$$

and

$$\beta\hbar S_{ss}[\mathbf{p}_j] = {}^1/_2\sum_{j,k,n} (\alpha^{(n)})^{-1}\mathbf{p}_{jn}\cdot(\mathbf{1} - \alpha^{(n)}\tilde{\mathbf{T}})_{jk}\cdot\mathbf{p}^*_{kn} - \sum_{j,k,n} \mathbf{p}_{jn}\cdot[\delta_{n0}(\mathbf{T}_{j0}\cdot\mathbf{m}_0 + \tilde{\mathbf{T}}_{jk}\cdot\mathbf{m}_k) + \mathbf{T}_{j0}\cdot\mathbf{p}^*_{0n}] - {}^1/_2\sum_{jk} \mathbf{m}_j\cdot\tilde{\mathbf{T}}_{jk}\cdot\mathbf{m}_k \tag{A3}$$

In eqs A2 and A3 $\mathbf{p}_{0n}$ and $\mathbf{p}_{jn}$ are the Fourier amplitudes of the Euclidean paths $\mathbf{p}_j(\tau)$ and $\mathbf{p}_0(\tau)$ on the time interval $\beta\hbar$, e.g.

$$\mathbf{p}_{0n} = \int_0^{\beta\hbar} \mathbf{p}_j(\tau)\exp(i\omega_n\tau)\,d\tau \tag{A4}$$

where $\omega_n = 2\pi n/\beta\hbar$ is the boson Matsubara frequency. Also, in eqs A2 and A3

$$\alpha^{(n)}_{0i} = \alpha_{0i}\omega_0^2/(\omega_0^2 + \omega_n^2) \tag{A5}$$

and

$$\alpha^{(n)} = \alpha\omega_s^2/(\omega_s^2 + \omega_n^2) \tag{A6}$$

The path integrals over the trajectories $\mathbf{p}_j(\tau)$ and $\mathbf{p}_0(\tau)$ reduce to simple Gaussian integrals by the Fourier transformation to the amplitudes $\mathbf{p}_{jn}$ and $\mathbf{p}_{0n}$. This integration leads to the instantaneous energies given by eq 10 with E_{ss} as follows

$$E_{ss} = U_{ss}^{rep} + U_{ss}^{disp} - {}^1/_2 \sum_{j,k} \mathbf{m}_j \cdot \tilde{\mathbf{T}}_{jk} \cdot \mathbf{m}'_k \qquad \text{(A7)}$$

where

$$\mathbf{m}'_j = \mathbf{m}_j + \sum_{k,m} \alpha(\mathbf{1} - \alpha\tilde{\mathbf{T}})_{jk}^{-1} \cdot \tilde{\mathbf{T}}_{km} \cdot \mathbf{m}_m \qquad \text{(A8)}$$

is the effective dipole of the polarizable solvent molecules, U_{ss}^{disp} is the solvent−solvent dispersion potential. The solute−solvent component of E_i is given by eq 13 with

$$\mathbf{R}_p = \sum_j \mathbf{T}_{0j} \cdot \mathbf{m}'_j \qquad \text{(A9)}$$

and

$$\mathbf{R}_\infty = \sum_{jk} \mathbf{T}_{0j} \cdot \alpha(\mathbf{1} - \alpha\tilde{\mathbf{T}})_{jk}^{-1} \cdot \mathbf{T}_{k0} \qquad \text{(A10)}$$

Appendix B

Here we calculate the integral in eq 22 with the exponential function given by eq 39 at $\Delta\tilde{\alpha} > 0$. A negative polarizability variation is treated analogously. The integral is calculated by the Taylor series expansion of $\exp[F_i(\xi,X)]$ in $\Delta_i\xi\xi_i/(\xi + i\xi_i)$ (eq 39). This yields a series of integrals each containing a pole of order n. Their evaluation gives for the integral in eq 22, denoted as I_i, the following expression

$$I_i = \Delta_i A_i \sum_{n=0}^{\infty} \frac{(-\xi_i\Delta_i)^n}{(n+1)!n!} \frac{d^n}{d\xi_i^n}(\xi_i^{n+1} e^{-\xi_i Y}) \qquad \text{(B1)}$$

The derivatives in the above series can be recast in terms of Laguerre polynomials $L_n^1(x)$[41]

$$I_i = \xi_i\Delta_i A_i e^{-\xi_i Y} \sum_{n=0}^{\infty} \frac{(-\xi_i\Delta_i)^n}{(n+1)!} L_n^1(\xi_i Y) \qquad \text{(B2)}$$

This sum leads to eq 47 by using the identity[41]

$$J_\nu(2\sqrt{xz}) e^z (xz)^{-\nu/2} = \sum_{n=0}^{\infty} \frac{z^n}{\Gamma(n+\nu+1)} L_n^\nu(x) \qquad \text{(B3)}$$

where $J_\nu(x)$ and $\Gamma(x)$ are the Bessel and gamma functions, respectively.

References and Notes

(1) (a) Marcus, R. A. *J. Chem. Phys.* **1965**, *43*, 1261. (b) Marcus, R. A. *Annu. Rev. Phys. Chem.* **1964**, *15*, 155. (c) Marcus, R. A. *Rev. Mod. Phys.* **1993**, *65*, 599.

(2) (a) Newton, M. D.; Sutin, N. *Annu. Rev. Phys. Chem.* **1984**, *35*, 437. (b) Marcus, R. A.; Sutin, N. *Biochim. Biophys. Acta* **1985**, *811*, 265. (c) Barbara, P. F.; Meyer, T. J.; Ratner, M. A. *J. Phys. Chem.* **1996**, *100*, 13148. (d) Chen, P.; Meyer, T. J. *Chem. Rev.* **1998**, *98*, 1439.

(3) (a) Matyushov, D. V.; Schmid, R. *Mol. Phys.* **1995**, *84*, 533. (b) Matyushov, D. V.; Schmid, R. *J. Chem. Phys.* **1995**, *103*, 2034. (c) Matyushov, D. V. *Chem. Phys.* **1996**, *211*, 47. (d) Matyushov, D. V.; Schmid, R.; Ladanyi, B. M. *J. Phys. Chem. B* **1997**, *101*, 1035. (e) Vath, P.; Zimmt, M. B.; Matyushov, D. V.; Voth, G. A. *J. Phys. Chem. B* **1999**, *103*, 9130.

(4) Ando, K. *J. Chem. Phys.* **1997**, *107*, 4585.

(5) Kumar, P. V.; Maroncelli, M. *J. Chem. Phys.* **1995**, *103*, 3038.

(6) Onsager, L. *J. Am. Chem. Soc.* **1936**, *58*, 1486.

(7) (a) Böttcher, C. J. F. *Theory of Electric Polarization*; Elsevier: Amsterdam, 1973; Vol. 1. (b) Liptay, W. In *Modern Quantum Chemistry, Part II*; Sinanoğlu, O., Ed.; Academic Press: New York, 1965.

(8) Bursulaya, B. D.; Kim, H. J. *J. Phys. Chem.* **1996**, *100*, 16451.

(9) Frequencies of the solvent dynamic response for solutes with polarizabilities different in the ground and excited states have been reported in: Bursulaya, B. D.; Zichi, D. A.; Kim, H. J. *J. Phys. Chem.* **1995**, *99*, 10069. The response frequency is not, however, directly related to the reorganization energy, see, e.g., refs 5 and 8.

(10) (a) Pekar, S. I. *Research in Electronic Theory of Crystals*; USAEC: Washington, DC, 1963. (b) Kim, H. J.; Hynes, J. T. *J. Chem. Phys.* **1992**, *96*, 5088. (c) Gehlen, J. N.; Chandler, D.; Kim, H. J.; Hynes, J. T. *J. Phys. Chem.* **1992**, *96*, 1748. (d) Kim, H. J. *J. Chem. Phys.* **1996**, *105*, 6818, 6833. (e) Jeon, J.; Kim, H. J. *J. Chem. Phys.* **1997**, *106*, 5979. (f) Matyushov, D. V.; Ladanyi, B. M. *J. Chem. Phys.* **1998**, *108*, 6362. (g) Matyushov, D. V.; Ladanyi, B. M. *J. Phys. Chem. A* **1998**, *102*, 5027.

(11) (a) Lax, M. *J. Chem. Phys.* **1952**, *20*, 1752. (b) Warshel, A. *J. Phys. Chem.* **1982**, *86*, 2218. (c) Tachiya, M. *J. Phys. Chem.* **1989**, *93*, 7050. (d) Warshel, A.; Parson, W. W. *Annu. Rev. Phys. Chem.* **1991**, *42*, 279. (e) King, G.; Warshel, A. *J. Chem. Phys.* **1990**, *93*, 8682.

(12) (a) Gorodyskii, A. V.; Karasevskii, A. I.; Matyushov, D. V. *J. Electroanal. Chem.* **1991**, *315*, 9. (b) Matyushov, D. V. *Mol. Phys.* **1993**, *79*, 795. (c) Perng, B.-C.; Newton, M. D.; Raineri, F. O.; Friedman, H. L. *J. Chem. Phys.* **1996**, *104*, 7153, 7177.

(13) (a) Warshel, A.; Hwang, J.-K. *J. Chem. Phys.* **1986**, *84*, 4938. (b) Kuharski, R. A.; Bader, J. S.; Chandler, D.; Sprik, M.; Klein, M. L.; Impey, R. W. *J. Chem. Phys.* **1988**, *89*, 3248. (c) Marchi, M.; Gehlen, J. N.; Chandler, D.; Newton, M. *J. Am. Chem. Soc.* **1993**, *115*, 4178. (d) Zhou, H.-X.; Szabo, A. *J. Chem. Phys.* **1995**, *103*, 3481. (e) Yelle, R. B.; Ichiye, T. *J. Phys. Chem. B* **1997**, *101*, 4127.

(14) (a) Pratt, L. R. *Mol. Phys.* **1980**, *40*, 347. (b) Thompson, M. J.; Schweizer, K. S.; Chandler, D. *J. Chem. Phys.* **1982**, *76*, 1128. (c) Høye, J. S.; Stell, G. *J. Chem. Phys.* **1980**, *73*, 461. (d) Chen, Y.-C.; Lebowitz, J. L.; Nielaba, P. *J. Chem. Phys.* **1989**, *91*, 340. (d) Cao, J.; Berne, B. J. *J. Chem. Phys.* **1993**, *99*, 2902.

(15) For example: Kleinert, H. *Path integrals in quantum mechanics, statistics, and polymer physics*; World Scientific: Singapore, 1995; Chapter 2.

(16) The description in ref 10 was focused on the solute−solvent dispersion term $U_{0s,i}^{disp}$ in eq 10. The renormalization of the permanent dipoles by the solute and solvent polarizabilities was omitted. The exact result of integrating over the solute and solvent induced dipoles in eq 3 is given by eq 10.

(17) Simon S. H.; Dobrosavljević, V.; Stratt, R. M. *J. Chem. Phys.* **1990**, *93*, 2640.

(18) (a) Wasielewski, M. R.; Niemczyk, M. P.; Svec, W. A.; Pewitt, E. B. *J. Am. Chem. Soc.* **1985**, *107*, 1080. (b) Asahi, T.; Ohkohchi, M.; Matsusaka, R.; Mataga, N.; Zhang, R. P.; Osuka, A.; Maruyama, K. *J. Am. Chem. Soc.* **1993**, *115*, 5665. (c) Heitele, H.; Pöllinger, F.; Häberle, T.; Michel-Beyerle, M. E.; Staab, H. A. *J. Phys. Chem.* **1994**, *98*, 7402.

(19) (a) Miller, J. R.; Calcaterra, L. T.; Closs, G. L. *J. Am. Chem. Soc.* **1984**, *106*, 3047. (b) Jayanthi, S. S.; Ramamurthy, P. *J. Phys. Chem. A* **1997**, *101*, 2016.

(20) (a) Gaines, G. L.; O'Neil, M. P.; Svec, W. A.; Niemczyk, M. P.; Wasielewski, M. R. *J. Am. Chem. Soc.* **1991**, *113*, 719. (b) Häberle, T.; Hirsch, J.; Pöllinger, F.; Heitele, H.; Michel-Beyerle, M. E.; Anders, C.; Döhling, A.; Krieger, C.; Rückemann, A.; Staab, H. A. *J. Phys. Chem.* **1996**, *100*, 18269.

(21) (a) Khundkar, L. R.; Stiegman, A. E.; Perry, J. W. *J. Phys. Chem.* **1990**, *94*, 1224. (b) Biswas, M.; Nguyen, P.; Marder, T. B.; Khundkar, L. R. *J. Phys. Chem. A* **1997**, *101*, 1689.

(22) Gould, I. R.; Noukakis, D.; Gomez-Jahn, L.; Goodman, J. L.; Farid, S. *J. Am. Chem. Soc.* **1993**, *115*, 4405.

(23) Matyushov, D. V.; Ladanyi, B. M. *J. Chem. Phys.* **1997**, *107*, 1375.

(24) (a) Renge, I. *Chem. Phys.* **1992**, *167*, 173. (b) Liptay, W.; Wortmann, R.; Schaffrin, H.; Burkhard, O.; Reitinger, W.; Detzer, N. *Chem. Phys.* **1988**, *120*, 429. (c) Liptay, W.; Wortmann, R.; Böhm, R.; Detzer, N. *Chem. Phys.* **1988**, *120*, 439. (d) Wortmann, R.; Elich, K.; Lebus, S.; Liptay, W.; Borowicz, P.; Grabowska, A. *J. Phys. Chem.* **1992**, *96*, 9724.

(25) Liu, Y.-P.; Newton, M. D. *J. Phys. Chem.* **1995**, *99*, 12382.

(26) (a) Englman, R.; Jortner, J. *Mol. Phys.* **1970**, *18*, 145. (b) Kestner, N. R.; Logan, J.; Jortner, J. *J. Phys. Chem.* **1974**, *21*, 2148.

(27) (a) Walker, G. C.; Åkesson, E.; Johnson, A. E.; Levinger, N. E.; Barbara, P. F. *J. Phys. Chem.* **1992**, *96*, 3728. (b) Cortés, J.; Heitele, H.; Jortner, J. *J. Phys. Chem.* **1994**, *98*, 2527. (c) Bixon, M.; Jortner, J.; Cortes, J.; Heitele, H.; Michel-Beyerle, M. E. *J. Phys. Chem.* **1994**, *98*, 7289. (d) Claude, J. P.; Williams, D. S.; Meyer, T. J. *J. Am. Chem. Soc.* **1996**, *118*, 9782.

(28) Fischer, G. *Vibronic Coupling. The Interaction between the Electronic and Nuclear Motions*; Academic Press: London, 1984.

(29) (a) Kubo, R.; Toyozawa, Y. *Prog. Theor. Phys.* **1955**, *13*, 160. (b) Lin, S. H. *J. Chem. Phys.* **1966**, *44*, 3759. (c) Riseborough, P. S. *Ann. Phys.* **1984**, *153*, 1. (d) Skinner, J. L.; Hsu, D. *J. Phys. Chem.* **1986**, *90*, 4931. (e) Tang, J. *Chem. Phys.* **1994**, *188*, 143. (f) Reichman, D.; Silbey, R. J.; Suárez, A. *J. Chem. Phys.* **1996**, *105*, 10500.

(30) (a) Kakitani, T.; Mataga, N. *J. Phys. Chem.* **1985**, *89*, 8. (b) Kakitani, T.; Mataga, N. *J. Phys. Chem.* **1985**, *89*, 4752. (c) Kakitani, T.; Matsuda, N.; Yoshimori, A.; Mataga, N. *Prog. React. Kinet.* **1995**, *20*, 347.

(31) Tachiya, M. *Chem. Phys. Lett.* **1989**, *159*, 505.

(32) (a) Liptay, W. In *Excited States*; Lim, E. C., Ed.; Academic Press: New York, 1974; Vol. 1. (b) Reimers, J. R.; Hush, N. S. *J. Phys. Chem.* **1991**, *95*, 9773. (c) Karki, L.; Lu, H. P.; Hupp, J. T. *J. Phys. Chem.* **1996**, *100*, 15637. (d) Karki, L.; Hupp, J. T. *J. Am. Chem. Soc.* **1997**, *119*, 4070. (e) Bublitz, G. U.; Laidlaw, W. M.; Denning, R. G.; Boxer, S. G. *J. Am. Chem. Soc.* **1998**, *120*, 6068.

(33) (a) Stanton, J. F.; Gauss, J. *J. Chem. Phys.* **1996**, *104*, 9859. (b) Jonsson, D,; Norman, P.; Ågren, H. *Chem. Phys.* **1997**, *224*, 201. (c) Hättig, C.; Christiansen, O.; Coriani, S.; Jørgensen, P. *J. Chem. Phys.* **1998**, *109*, 9237.

(34) (a) Andersson, P. O.; Gillbro, T.; Ferguson, L.; Cogdell, R. J. *Photochem. Photobiol.* **1991**, *54*, 353. (b) Bublitz, G. U.; Ortiz, R.; Runser, C.; Fort, A.; Barzoukas, M.; Marder, S. R.; Boxer, S. G. *J. Am. Chem. Soc.* **1997**, *119*, 3365.

(35) (a) Carter, E. A.; Hynes, T. J. *J. Phys. Chem.* **1989**, *93*, 2184. (b) Carter, E. A.; Hynes, T. J. *J. Chem. Phys.* **1991**, *94*, 5961. (c) Fonseca, T.; Ladanyi, B. M.; Hynes, J. T. *J. Phys. Chem.* **1992**, *96*, 4085. (d) Åqvist, J.; Hansson, T. *J. Phys. Chem.* **1996**, *100*, 9512. (e) Matyushov, D. V.; Ladanyi, B. M. *J. Chem. Phys.* **1999**, *110*, 994.

(36) Tachiya, M.; Murata, S. *J. Am. Chem. Soc.* **1994**, *116*, 2434.

(37) (a) Asahi, T.; Mataga, N. *J. Phys. Chem.* **1989**, *93*, 6575. (b) Segawa, H.; Takehara, C.; Honda, K.; Shimidzu, T.; Asahi, T.; Mataga, N. *J. Phys. Chem.* **1992**, *96*, 503. (c) Benniston, A. C.; Harriman, A.; Philp, D.; Stoddart, J. F. *J. Am. Chem. Soc.* **1993**, *115*, 5298. (d) Hirsch, T.; Port, H.; Wolf, H. C.; Miehlich, B.; Effenberger, F. *J. Phys. Chem. B* **1997**, *101*, 4525. (e) Tétreault, N.; Muthyala, R. S.; Liu, R. S. H.; Steer, R. P. *J. Phys. Chem. A* **1999**, *103*, 2524.

(38) (a) Kober, E. M.; Caspar, J. V.; Lumpkin, R. S.; Meyer, T. J. *J. Phys. Chem.* **1986**, *90*, 3722. (b) Worl, L. A.; Duesing, R.; Chen, P.; Ciana, L. D.; Meyer, T. J. *J. Chem. Soc., Dalton Trans.* **1991**, 849. (c) Claude, J. D.; Meyer, T. J. *J. Phys. Chem.* **1995**, *99*, 51.

(39) (a) Hubig, S. M.; Kochi, J. K. *J. Phys. Chem.* **1995**, *99*, 17578. (b) Asahi, T.; Matsuo, Y.; Masuhara, H.; Koshima, H. *J. Phys. Chem. A* **1997**, *101*, 612.

(40) Birks, J. B. *Photophysics of Aromatic Molecules*; Wiley: London, 1970.

(41) Gradshteyn, I. S.; Ryzhik, I. M. *Tables of Integrals, Series, and Products*; Academic Press: San Diego, CA, 1994; pp 1061−1063.